J Sol-Gel Sci Technol (2018) 85:585–594
DOI 10.1007/s10971-017-4545-2

ORIGINAL PAPER: NANO-STRUCTURED MATERIALS (PARTICLES, FIBERS, COLLOIDS, COMPOSITES, ETC.)

Selective synthesis of scheelite/perovskite $CdWO_4$ nanoparticles: a mechanistic investigation of phase formation and property correlation

H. Eranjaneya[1] · G. T. Chandrappa[1]

Received: 19 August 2017 / Accepted: 10 November 2017 / Published online: 29 November 2017

Abstract We proposed a simple solution combustion strategy to fabricate $CdWO_4$ nanoparticles for the first time in two different polymorphs: a stable monoclinic and metastable tetragonal phase. The selective synthesis of polymorphs has been achieved by optimizing oxidizer to fuel ratio. Influence of oxidizer to fuel ratio on the formation of $CdWO_4$ polymorphs is of particular relevance to this study and the significant effects are discussed. A mechanistic comparison of properties between two phases has been carried out. Rietveld analyzes of powder X-ray diffraction patterns were performed using GSAS program. Transmission electron microscope images of as synthesized products show the particle sizes of *t*-$CdWO_4$ (10–20 nm) are smaller than the particle size of *m*-$CdWO_4$ (≈30 nm). The specific surface area was found to be 12 and 25 m^2/g for tetragonal and monoclinic phases, respectively. Photocatalytic activities were investigated by the degradation of methylene blue solution under UV light irradiation. It was found that the photocatalytic activity of tetragonal phase was higher than monoclinic phase, this can be attributed to smaller particle size and active sites of the catalyst that rely sensitively on synthetic conditions. We also explored the photoluminescence (PL) properties of *t*-$CdWO_4$ and compared with the PL results of *m*-$CdWO_4$.

Graphical abstract

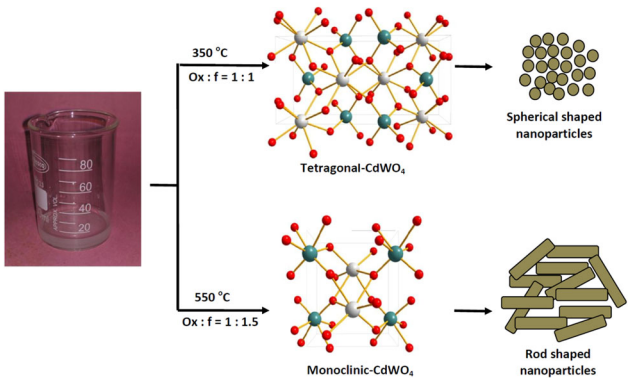

Keywords Nanoparticles · Combustion synthesis · Polymorphism · Cadmium tungstate · Photocatalytic activity

1 Introduction

Multicomponent metal oxides such as metal tungstates (WO_4^{2-}) and molybdates (MoO_4^{2-}), have been studied extensively owing to their intriguing physical and chemical properties. Particularly AMO_4 type oxides (A = Zn, Cd, Pb, and Cs, M = W and Mo), draw the attention of researchers for their wide range of applications in photoluminescence [1], scintillators [2], photochromism [3], multiferroic materials [4], and photocatalysis [5–7]. The divalent metal tungstates and molybdates with small A^{2+} ion (radius ≤0.77 Å: Mg, Mn, Fe, Co, Ni, Cu, and Zn) crystallizes in wolframite type structures and with large A^{2+} ion (radius

Electronic supplementary material The online version of this article (https://doi.org/10.1007/s10971-017-4545-2) contains supplementary material, which is available to authorized users.

✉ G. T. Chandrappa
gtchandrappa@yahoo.co.in

[1] Department of Chemistry, Central College Campus, Bangalore University, Bengaluru 560001, India

≥0.99 Å: Ca, Sr, Ba, and Pb) crystallizes in scheelite type structures. Being an intermediate, cadmium tungstate (radius of $Cd^{2+} = 0.97$ Å) crystallizes in both the polymorphs: stable wolframite (monoclinic) and a metastable scheelite (tetragonal) structures. The structural factors such as order–disorder in the lattice will strongly influence the physical and chemical properties of materials [8], hence $CdWO_4$ gains significant interests in scientific community owing to its ability of exhibiting different polymorphs. Also, recent reports prove that $CdWO_4$ has caught the attention of scientists and technologists as photocatalyst for water splitting and/or degradation of organic contaminants under UV light irradiation [9–12]. On account of this, synthesis of $CdWO_4$ and precise control of the polymorphs is significantly important. In this regard, several reports were found for the synthesis of $CdWO_4$ crystals with stable monoclinic structure, because of their high average refractive index, excellent X-ray absorption coefficient, high stopping power, and low radiation damage [13–15]. On the other hand, owing to difficulty in its preparation, limited number of reports were found for the synthesis of tetragonal $CdWO_4$. For the first time, Rondinone et al. have synthesized the tetragonal $CdWO_4$ stabilized by propylene glycol by solvothermal method at 200 °C for 10 h followed by several times washing and they found that it converts back to the monoclinic wolframite phase between 300 and 500 °C [16]. Similarly, Li et al. have described the synthesis of $CdWO_4$ polymorphs in both tetragonal and monoclinic phases via hydrothermal method for 10 h and it has been utilized for the degradation of methyl orange dye using ultraviolet (UV) light irradiation under optimized conditions [10]. Furthermore, Sofronov et al. have reported the microwave synthesis of polymorphic $CdWO_4$ mixture and maximum concentration of tetragonal phase (about 70%) was observed during decomposition of initial components mixture in vacuum conditions [17]. The above said synthetic methods for the fabrication of either monoclinic or tetragonal $CdWO_4$ have many draw backs such as long reaction time, multistep process, high calcination temperatures, and/or special experimental arrangements. On account of this, there is a critical need to discover novel synthetic way that allows the quick and inexpensive fabrication of nanoscale materials with desired phase composition. Solution combustion synthesis (SCS) is an exciting phenomenon, which involves propagation of rapid self-sustained exothermic reactions along an aqueous media and offers an exceptional solution to the above mentioned synthetic complexities [18]. The SCS method has been employed for the synthesis of several meta-stable phases by the present authors. To quote a few are: a unique approach for synthesizing VO_2 using a solution combustion process which eliminates the use of an inert atmosphere in the synthesis, thereby significantly reducing the complexity of handling the reaction [19]. A nanocrystalline monoclinic-$BiVO_4$ photocatalyst for H_2 evolution, has been synthesized by a facile solution combustion synthesis [20].

In this paper, a facile one-step SCS route has been developed for the selective fabrication of polymorphous $CdWO_4$ nanopowder by tweaking oxidizer to fuel ratio. To the best of our knowledge, we are the first to establish a simple and unique solution combustion reaction for the synthesis of $CdWO_4$ nanopowder in monoclinic and tetragonal phases. Rietveld refinement of PXRD data has been performed using the computer program 'General Structure Analysis System' (GSAS). The photocatalytic properties of both the polymorphs were evaluated by degradation of methylene blue dye under UV light irradiation and the influence of particle size on photocatalytic activity has been discussed.

2 Experimental section

2.1 Sample preparation

All chemicals were purchased from Merck Ltd. and used without further purification. Synthesis of $CdWO_4$ in two different polymorphs has been achieved through solution combustion approach by tuning oxidizer/fuel ratio at different temperatures. An aqueous solution of peroxotungstic acid as tungsten source was prepared by dissolving tungsten powder in 30% solution of H_2O_2 by heating at 60 °C for 20 min.

2.1.1 Synthesis of tetragonal $CdWO_4$

Precursor solution containing stoichiometric ratios of peroxotungstic acid solution, $Cd(NO_3)_2{\cdot}4H_2O$ (W:Cd = 1:1) and sucrose as fuel (Oxidizer:fuel = 1:1) was prepared by dissolving all the components. In a typical reaction 0.2 g tungsten powder (5 mL H_2O_2), 0.3355 g cadmium nitrate and 0.0775 g sucrose were used. The obtained solution was pre-heated on a hot plate until viscous gel formed then placed in a muffle furnace at 350 °C. Within a minute, the precursor solution expands to form a froth to give voluminous white powder which was immediately removed from the furnace to avoid the formation of monoclinic phase as impurity.

2.1.2 Synthesis of monoclinic $CdWO_4$

In a typical reaction 0.2 g tungsten powder (5 mL H_2O_2), 0.3355 g cadmium nitrate and 0.1163 g sucrose (Oxidizer: fuel = 1:1.5) were mixed to obtain homogeneous precursor solution. The obtained reactant mixture was pre-heated on a hot plate until viscous gel formed then it is placed in a

furnace at 550 °C. A voluminous mass obtained which undergoes smoldering combustion to give black mass due to excess fuel. The obtained black mass was calcined at same temperature for 15 min to obtain pure *m*-$CdWO_4$.

2.2 Characterization

The powder X-ray diffraction (PXRD) measurements were performed on a PANalytical X'pert PRO MPD instrument with graphite-filtered CuKα radiation source ($\alpha = 1.541$ Å). Surface morphology and micro-structural studies of $CdWO_4$ nanopowder were carried out using a scanning electron microscope (SEM) (VEGA3 TESCAN) and transmission electron microscope (TEM) (JEOL JEM-2100). Nitrogen adsorption–desorption measurements were carried out at 77 K using a gas sorption analyzer (Quantachrome Corporation NOVA 1000). UV–Vis measurements were performed using a UV–Vis spectrophotometer (Shimadzu 3101). Fourier transform infrared (FTIR) spectrum of the product were recorded using Bruker Alpha-P spectrometer (ATR mode, diamond crystal, 400–4000 cm^{-1}). The room temperature photoluminescence (PL) study was carried out on a Perkin-Elmer LS-55 luminescence spectrometer using Xe lamp with an excitation wavelength of 325 nm at room temperature.

2.3 Photocatalytic test

An aqueous suspension (200 mL) containing 8 mg/L methylene blue and 200 mg of as-prepared samples were placed in a glass beaker. To establish the adsorption/desorption equilibrium the suspensions were magnetically stirred before illumination in the dark for 30 min at room temperature. The photocatalytic activity was determined by illuminating the suspensions with ultraviolet light from a Hg lamp. At a given time intervals 3 mL of the sample solution was taken out and separated by centrifugation. The supernatants were analyzed by recording variations in the absorption band maximum (664 nm for MB) using a UV-3101 PC UV–VIS–NIR scanning spectrophotometer (Shimadzu).

3 Results and discussion

In most of the previous attempts, $NaWO_4$ has been used as source of tungsten for $CdWO_4$ synthesis [21, 22]. For the first time we have used peroxo route, where tungsten metal powder was dissolved in H_2O_2 to form peroxotungstic acid. Advantage of peroxo route would be to avoid the presence/doping of foreign spectator ions such as Na^+ that will remain in the SCS derived final product even after thorough washing. For instance, tungstic acid aqueous solutions can be used via the acidification of tungstates, however, they are not stable and a crystalline precipitate of WO_3 is formed during the pre-heating stage of precursor solution. Based on the literature [23, 24], possible reactions for the formation of peroxotungstic acid [WO_2 (O_2) (OH_2)] solution is given by the following equations:

$$W + 3H_2O_2 \rightarrow H_2WO_4\,(aq) + 2H_2O$$

$$H_2WO_4 + H_2O_2 \rightarrow WO_2\,(O_2)\,(OH_2)\,(aq) + H_2O$$

Selective synthesis of tetragonal/monoclinic $CdWO_4$ phase was achieved using solution combustion approach by optimizing oxidizer to fuel ratio. SCS process is a rapid process where the reaction takes place abruptly and thus suitable for the synthesis of metastable phases [20]. The high thermal gradients and rapid cooling nature of SCS can give rise to new non-equilibrium or metastable phases. In SCS, actual temperature during the reaction is higher than furnace temperature due to the burning of fuel (an organic molecule). The magnitude of this temperature depends on the amount of fuel and oxidizer present in the precursor solution.

Several experiments were carried out to test the effect of oxidizer/fuel ratio on the phase composition at 450 °C. When oxidizer/fuel ratio is 1:1, the reaction occurs without the participation of oxygen from the air, because the initial aqueous solution contains a stoichiometric amount of oxidizer, also temperature produced is less and hence metastable *t*-$CdWO_4$ is formed. As the quantity of fuel increases the PXRD peaks corresponds to monoclinic phase starts appearing (Fig. 1) and when oxidizer/fuel ratio is 1:1.5, pure monoclinic phase is formed. In the later case (as fuel is surplus) the reaction occurs with the participation of oxygen from the air. Figure 1 shows the variation of PXRD patterns with the variation of oxidizer/fuel ratio at furnace

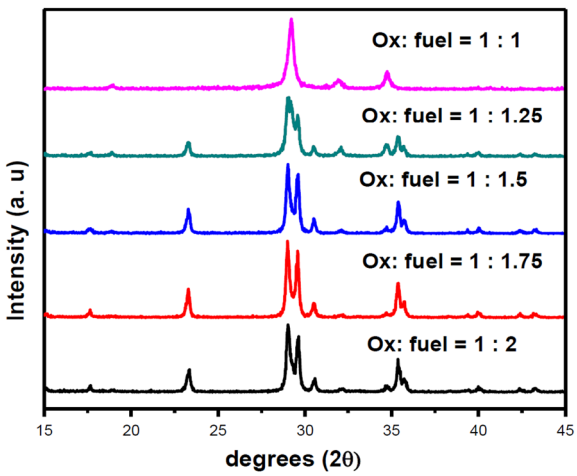

Fig. 1 Powder X-ray diffraction pattern of $CdWO_4$ polymorphs with different oxidizer to fuel ratio at 450 °C

temperature 450 °C. The overall redox reaction is given by the following scheme:

$$4Cd(NO_3)_2.4H_2O + 4WO_2(O_2)(OH_2) + C_{12}H_{22}O_{11} \rightarrow 4CdWO_4 + 31H_2O + 12CO_2 + 4N_2$$

In order to achieve the repeatability and purity of the tetragoanal and monoclinic phases, the furnace temperature has been maintained at 350 and 550 °C, respectively for the synthesis of pure polymorphs. Subsequently the same materials have been utilized for characterization and application studies.

3.1 Refinement and crystal structure of the polymorphs

The phase composition of the samples was determined by the Rietveld analysis of experimental PXRD patterns using general structure analysis system (GSAS) program. Initial atomic positions for refinement of tetragonal phase were adopted from a model tetragonal Scheelite $CdMoO_4$ (I 41/a) [25]. Figure 2a summarizes the results of refinement for tetragonal phase where the upper curve shows a solid (simulated) line overlaying the experimental data. Immediately below the experimental data are the reflection markers. At the bottom of the figure is the difference curve, indicating the reasonably good fit ($\chi^2 = 1.518$, $RF^2 = 0.0415$). Figure 2b corresponds to the results of refinement for monoclinic phase ($\chi^2 = 1.271$, $RF^2 = 0.0568$). The unit cell parameters as determined by Rietveld analysis for both phases are reported in Tables 1 and 2 summarizes the coordinate positions of each atom in the structure.

Crystal structures for both tetragonal and monoclinic cadmium tungstate were constructed using diamond software and presented in Fig. 3a, b. The structures have been developed using results of refinement such as structural parameters and atomic positions. In *t*-$CdWO_4$ structure (space group of I41/a (no.88), $Z = 4$), the coordination around tungsten ions is symmetrically tetrahedral, showing four W–O bonds with the same bond length of 1.902 Å. The overall coordination around cadmium ions is eight (Fig. 3a). Whereas in *m*-$CdWO_4$ structure (space group of P2/c (no.13), $Z = 4$), the coordination around both tungsten and cadmium ions is a distorted octahedra (Fig. 3b).

3.2 Nano-structural characterization

The morphology of the synthesized samples were characterized using SEM. Figure 4a, b shows the SEM images of tetragonal cadmium tungstate and Fig. 4c, d are the SEM images of monoclinic phase. The SEM images of tetragonal phase exhibits highly porous nature while the monoclinic phase exhibits some interesting morphology of uniform distribution of nanosized-rod-shaped particles, however the

Table 1 Unit cell parameters as obtained by Rietveld refinement

Phase	*a* (Å)	*b* (Å)	*c* (Å)	*β* (deg)
Tetragonal	5.1590	5.1590	11.1690	–
Monoclinic	5.02530	5.85669	5.07199	91.4893

Table 2 Atomic positions as obtained by Rietveld refinement

Phase	Atom	*x*	*y*	*z*	Occupancy
Tetragonal	W	0	0.25	0.625	1
	Cd	0.0	0.25	0.125	1
	O	0.226	−0.095	0.035	1
Monoclinic	W	0	0.18	0.25	1
	Cd	0.5	0.304	0.75	1
	O1	0.247	0.376	0.392	1
	O2	0.212	0.092	−0.04	1

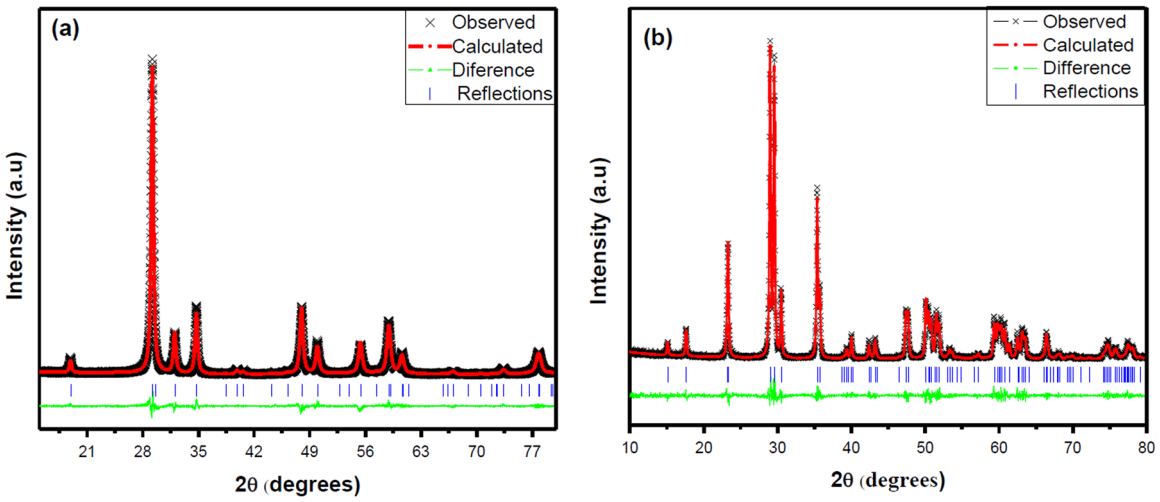

Fig. 2 Rietveld fit of a representative PXRD patterns of **a** tetragonal-$CdWO_4$ nanopowder and **b** monoclinic-$CdWO_4$ nanopowder

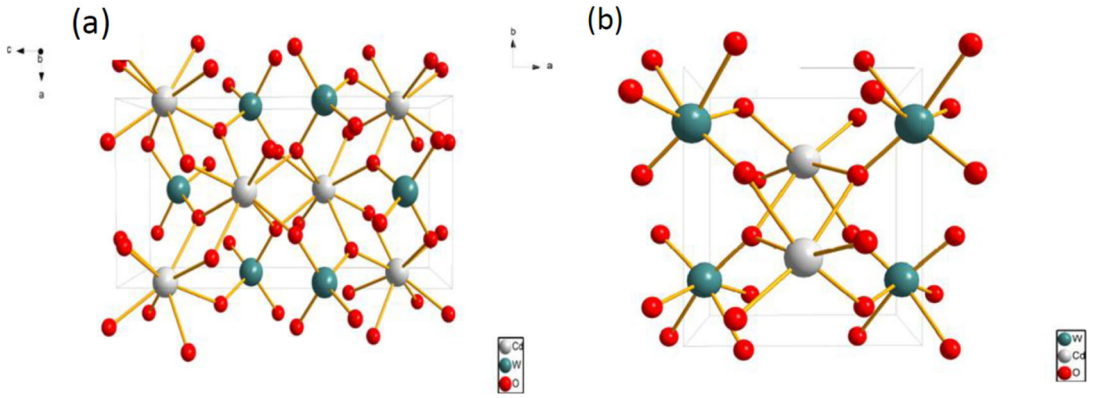

Fig. 3 Representation of **a** tetragonal structure for the $CdWO_4$ crystals formed by tetrahedral [WO_4] and deltahedral [CdO_8] clusters and **b** monoclinic structure for the $CdWO_4$ crystals formed by distorted octahedral [WO_6] and [CdO_6] clusters

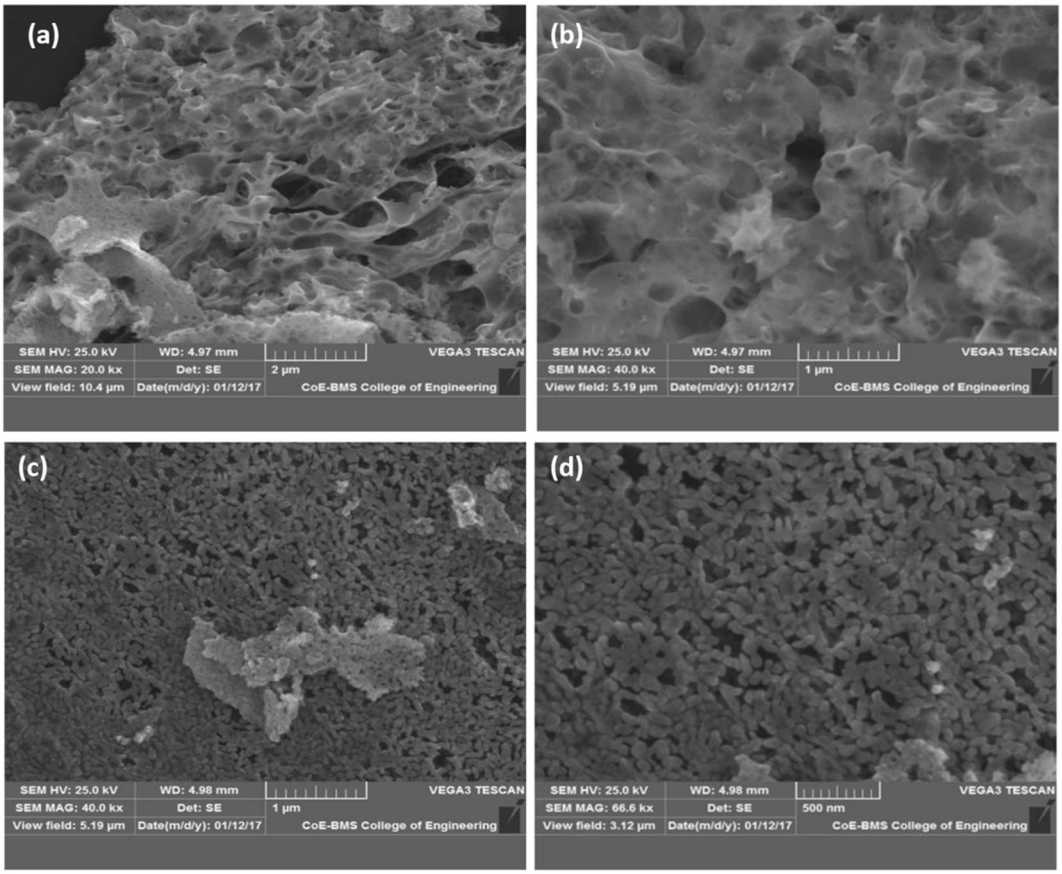

Fig. 4 SEM images of *t*-$CdWO_4$ nanopowder (**a**, **b**) and *m*-$CdWO_4$ nanopowder (**c**, **d**)

particles are rigidly joined together or agglomerated due to the calcination of the sample to remove excess carbon. The microscopic elemental analysis of the selected particles was checked by energy dispersive X-ray spectroscopy for both the phases (Fig. S1), which reveals the existence of Cd, W, and O elements. The morphology and structure of the nano polymorphs were further characterized by TEM and selected area electron diffraction (SAED) patterns. Figure 5a, b shows the TEM images of tetragonal sample containing well dispersed irregular shaped nanoparticles having the average size distribution ranging from 10 to 20 nm. HRTEM image (Fig. 5c) reveals that the lattice spacing of 0.46 nm corresponds to crystalline plane of tetragonal phase. The SAED pattern recorded from the [$1\bar{1}0$] zone axis shown in Fig. 5d reveals the single crystalline nature of the sample. Similar nano-structural characterizations have been

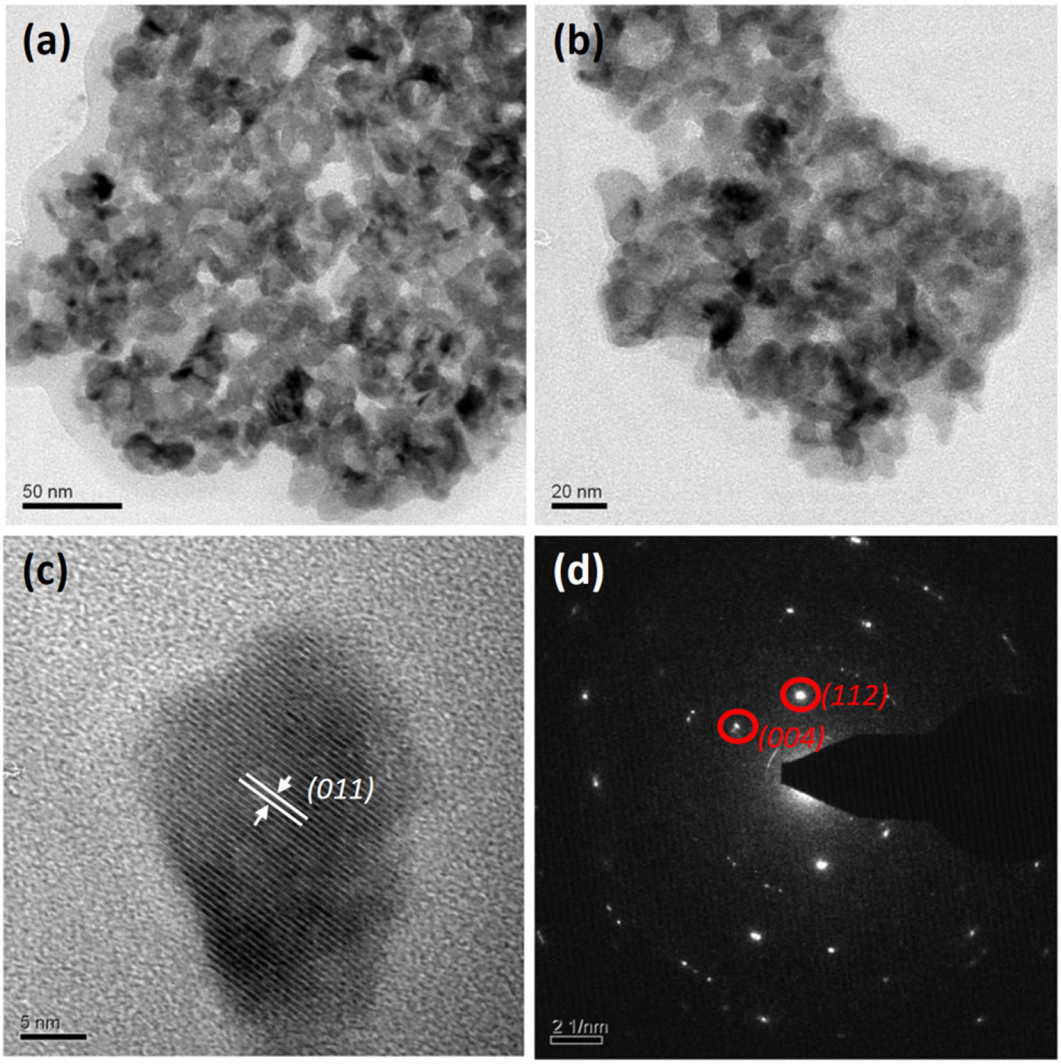

Fig. 5 TEM images (**a**, **b**), HRTEM image (**c**) and SAED pattern (**d**) of *t*-$CdWO_4$ nanopowder

carried out for monoclinic phase, Fig. 6a, b shows the TEM images of *m*-$CdWO_4$ containing nearly rod-shaped nanoparticles of dimensions in nano range (≈30 nm in width and 110 nm in length). The lattice spacing of 0.502 nm in HRTEM image (Fig. 6c) corresponds to *(100)* crystalline plane of monoclinic phase. The SAED pattern for *m*-$CdWO_4$ recorded from the [$\bar{1}$10] zone axis is presented in Fig. 6d and some of the bright spots are indexed to *(112)*, *(002)*, and *(110)* crystalline planes.

The nitrogen adsorption-desorption isotherms of polymorphic $CdWO_4$ sample are presented in Fig. 7a, b with an inset showing the pore size distribution. It is found that *t*-$CdWO_4$ shows representative type-IV isotherm (Fig. 7a) according to Brunauer–Deming–Deming–Teller classification [26]. In the region of 0.4–0.9 relative pressure, there is a large hysteresis loop of type H4. Figure 7b shows the nitrogen adsorption-desorption isotherm of *m*-$CdWO_4$, it represents the type-IV isotherm and H3 type hysteresis loop. The average pore diameter for *t*-$CdWO_4$ is found to be ~3.1 nm suggesting mesoporous nature with small amount of micropores and *m*-$CdWO_4$ with ~1.73 nm pore diameter suggesting microporous nature. The specific surface area of the sample was calculated using the Brunauer–Emmett–Teller (BET, nitrogen, 77 K) method and is found to be ~12 and ~25 m^2/g for tetragonal and monoclinic phases, respectively. In our investigation, *m*-$CdWO_4$ shows higher surface area despite having particles with larger size compared to *t*-$CdWO_4$. This anomaly could be explained based on porosity and pore diameter; since surface area depends not only on particle size but also on porosity, pore volume, and extent of aggregation or agglomeration of the nanomaterials. du Plessis reports that as pore size decreases, specific surface area of the materials increases [27]. As *m*-$CdWO_4$ exhibits smaller pore diameter (~1.73 nm)

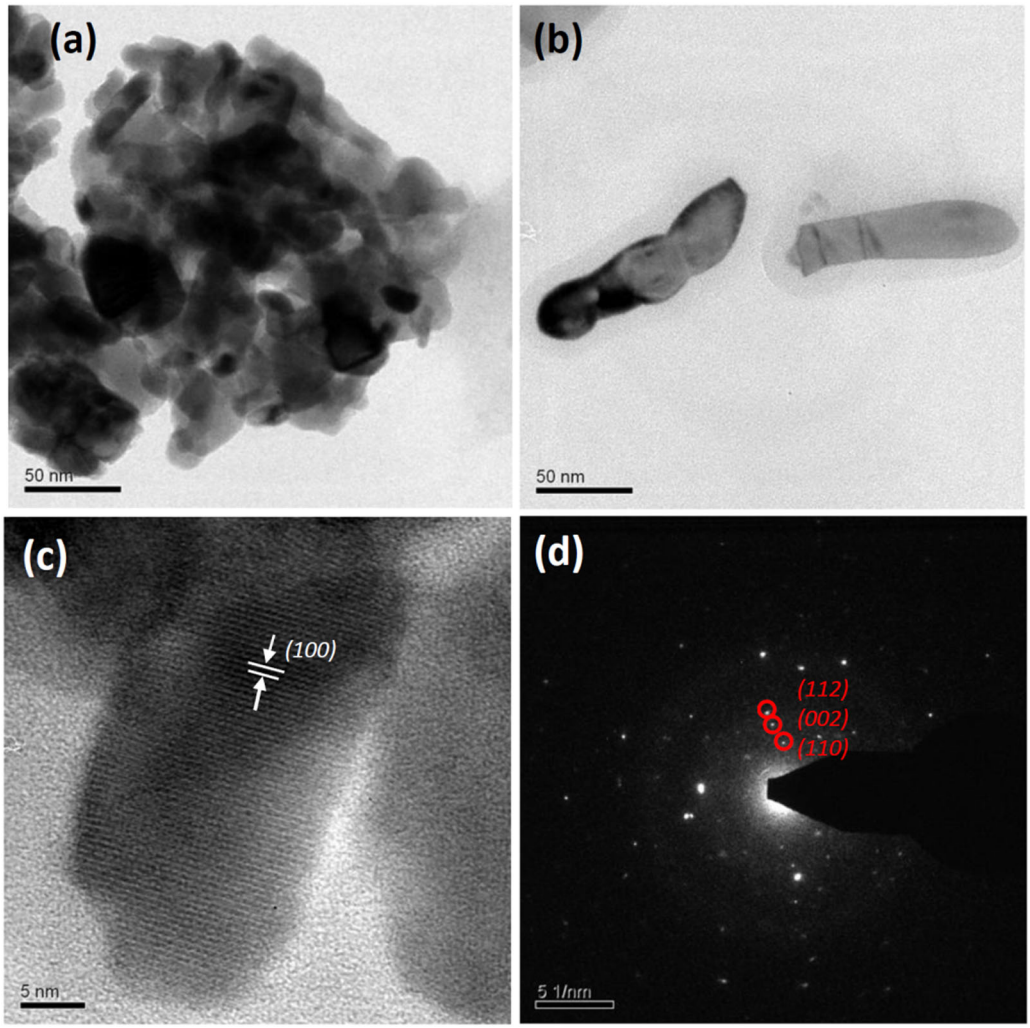

Fig. 6 TEM images (**a**, **b**), HRTEM image (**c**) and SAED pattern (**d**) of *m*-$CdWO_4$ nanopowder

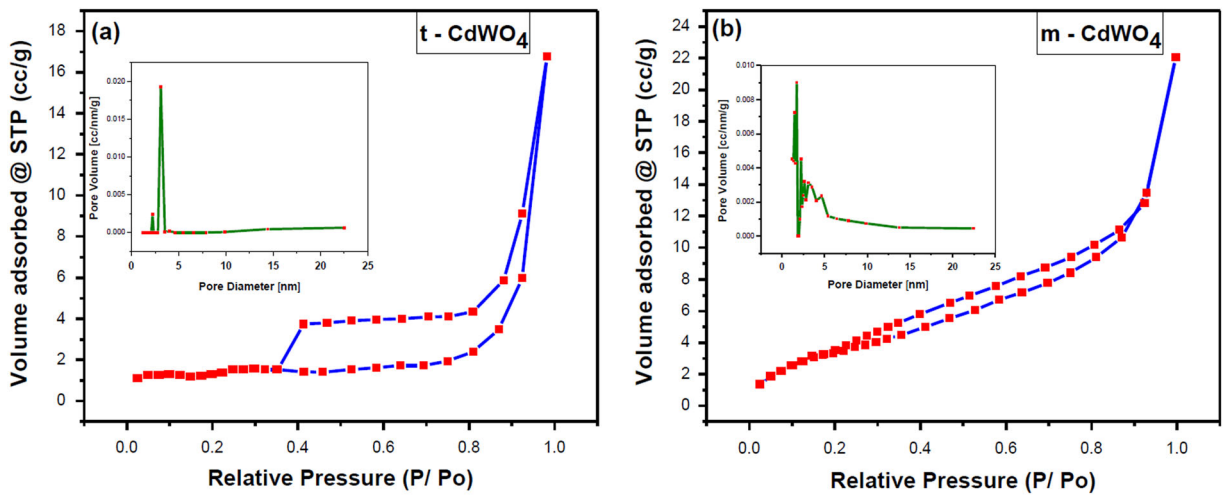

Fig. 7 Nitrogen adsorption–desorption isotherms and the corresponding pore-size distribution curves (inset) of **a** *t*-$CdWO_4$ and **b** *m*-$CdWO_4$ nanopowder

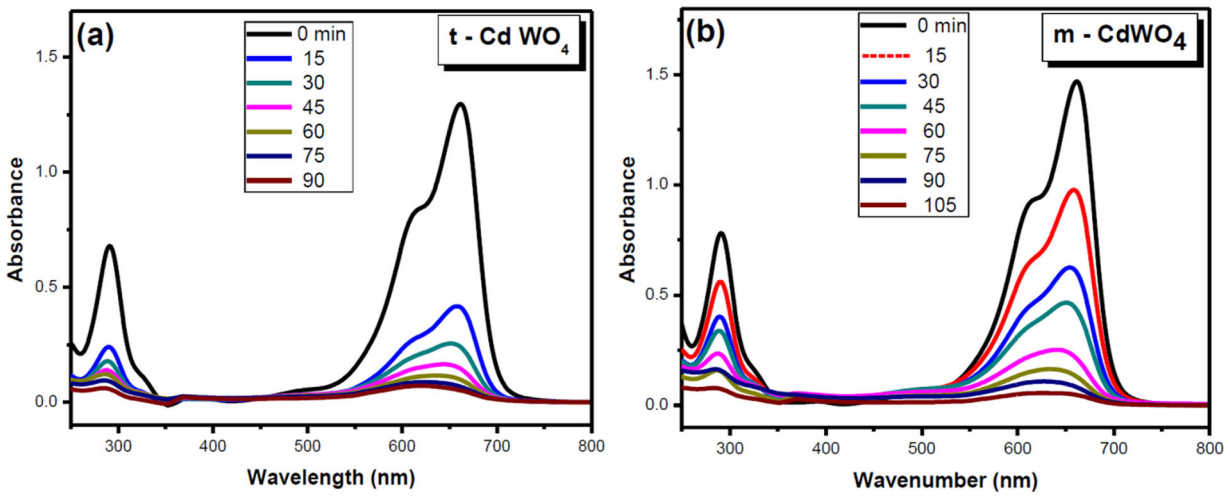

Fig. 8 The temporal evolution of the spectral changes during the photodegradation of methylene blue solution over **a** *t*-$CdWO_4$ and **b** *m*-$CdWO_4$ nanopowder

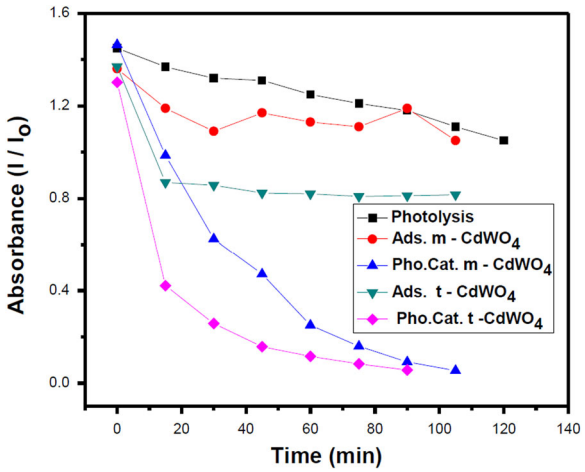

Fig. 9 Comparison of photodegradation efficiency of $CdWO_4$ polymorphs

compared to *t*-$CdWO_4$ (~3.1 nm); there is a possibility of having higher surface area for *m*-$CdWO_4$ than *t*-$CdWO_4$. High porosity of *m*-$CdWO_4$ can be attributed to fuel rich synthetic conditions, which enhances the porosity due to the release of large amount of gases during combustion reaction.

Decolorization of methylene blue (MB) was investigated for both the polymorphs. Two hundred milligram $CdWO_4$ nanopowder was dispersed in 200 mL of 8 ppm MB solution. Figure 8a shows the temporal evolution of spectral changes during photodegradation of 8 ppm MB solution in presence of tetragonal $CdWO_4$. Figure 8b shows the temporal evolution of spectral changes during photodegradation of 8 ppm MB solution in presence of monoclinic $CdWO_4$. Separate experiments were carried out to investigate the adsorption activity of the catalyst in dark and self photolysis of MB without catalyst. Figure 9 shows the comparison of photocatalytic activity of $CdWO_4$ polymorphs with adsorption activity of the catalyst and self photolysis of MB. It is evident that the self photolysis of MB under UV irradiation is negligible compared to photodegradation and also it shows that both irradiation and catalyst are necessary for the degradation of dye. It is found that 90% of the dye has been degraded in presence of tetragonal $CdWO_4$ in 60 min whereas, for monoclinic phase it requires 90 min for the 90% degradation of MB. The high photocatalytic activity of tetragonal phase is attributed to its small particle size (10–20 nm) compared to the particle size of monoclinic phase (≈30 nm in width and 110 nm in length). Further, the low photocatalytic activity of monoclinic phase is explained using PL results. The efficiency of photocatalyst depends on the generation of photo-induced electrons and separation of electron–hole pair. The rate of recombination of photo generated electron–hole pair can be related to PL emission intensity, since PL emission of semiconductors mainly arises from the charge carrier recombination [28]. In general, higher the recombination rate of electron-hole pairs, higher is the PL emission intensity, which indicates the lower photocatalytic properties of the photocatalyst [29]. The room temperature PL spectra of monoclinic cadmium tungstate (Fig. 10c, d) with the excited wavelength at 282 nm exhibits a broad and high intense emission peak centered at 473 nm, whereas tetragonal cadmium tungstate (Fig. 10a, b) with the excited wavelength at 310 nm exhibits a sharp and low intense emission peak at 424 nm. Hence, as the intensity of PL emission peak of monoclinic phase is very high as compared to intensity of PL emission peak of tetragonal phase, the monoclinic cadmium tungstate exhibits lower photocatalytic activity than the tetragonal cadmium tungstate.

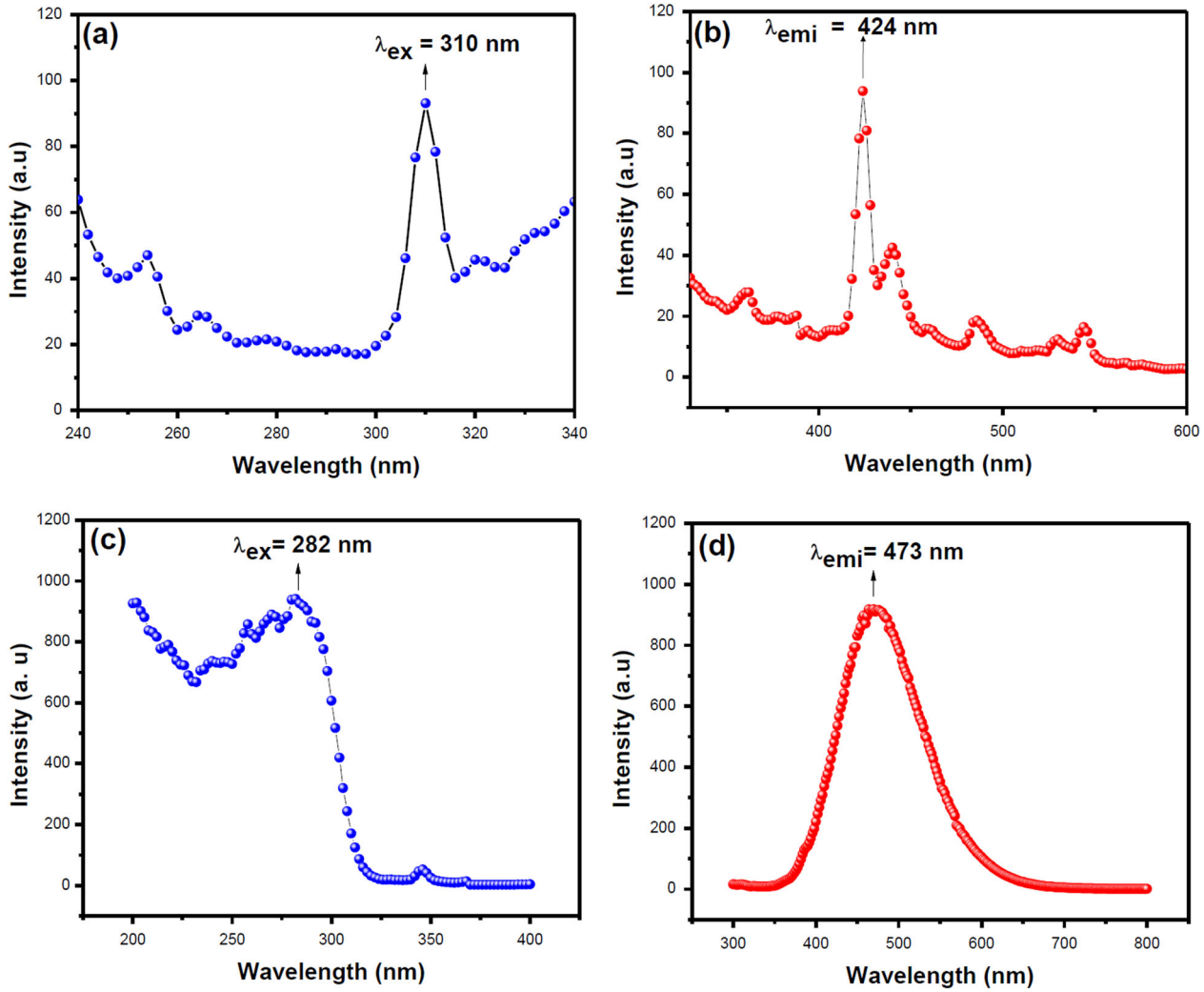

Fig. 10 Photoluminescence spectra of tetragonal $CdWO_4$ (**a**, **b**) and monoclinic $CdWO_4$ (**c**, **d**)

4 Conclusions

A simple, quick, and efficient solution combustion strategy has been developed for the syntheses of cadmium tungstate polymorphs. Precise control of polymorphic composition was achieved by tuning oxidizer to fuel ratio. Rietveld refinement of experimentally obtained PXRD patterns has been carried out using GSAS. Nanostructural characterization was carried out using SEM and TEM techniques and it is found that tetragonal $CdWO_4$ has small particle size compare to monoclinic $CdWO_4$. Photocatalytic activity of tetragonal phase is found to be higher than monoclinic phase for the degradation of methylene blue under UV light irradiation. Based on the results herein, we conclude that SCS is a time and energy efficient method to synthesize metastable phases.

Acknowledgements One of the authors, (HE) acknowledges the Council of Scientific and Industrial Research (CSIR), New Delhi, India, for awarding CSIR-SRF fellowship to carry out this research work and Dr. Ashoka S, Assistant professor, Dayanand Sagar University for useful suggestions and discussion in this research work.

Compliance with ethical standards

Conflict of interest The authors declare that they have no conflict of interests.

References

1. Su Y, Li L, Li G (2008) Synthesis and optimum luminescence of $CaWO_4$-based red phosphors with codoping of Eu^{3+} and Na^{+}. Chem Mater 20:6060–6067. https://doi.org/10.1021/cm8014435
2. Nikl M (2006) Scintillation detectors for x-rays. Meas Sci Technol 17:R37–R54. https://doi.org/10.1088/0957-0233/17/4/R01
3. Fukuda K, Akatsuka K, Ebina Y et al. (2008) Exfoliated nanosheet crystallite of cesium tungstate with 2D pyrochlore structure: synthesis, characterization, and photochromic properties. ACS Nano 2:1689–1695. https://doi.org/10.1021/nn800184w
4. Zhou YX, Zhang Q, Gong JY, Yu SH (2008) Surfactant-assisted hydrothermal synthesis and magnetic properties of urchin-like

MnWO4 microspheres. J Phys Chem C 112:13383–13389. https://doi.org/10.1021/jp804211w
5. Eranjaneya H, Chandrappa GT (2016) Solution combustion synthesis of nano $ZnWO_4$ photocatalyst. Trans Indian Ceram Soc 75:133–137. https://doi.org/10.1080/0371750X.2016.1181990
6. Li D, Bai X, Xu J, Zhu Y (2014) Synthesis of $CdWO_4$ nanorods and investigation of the photocatalytic activity. Phys Chem Chem Phys 16:212–218. https://doi.org/10.1039/c3cp53403k
7. Jiang YN, Liu BD, Yang WJ et al. (2016) New strategy for the in situ synthesis of single-crystalline $MnWO_4$ /TiO 2 photocatalysts for efficient and cyclic photodegradation of organic pollutants. CrystEngComm 18:1832–1841. https://doi.org/10.1039/C5CE02445E
8. Chandrappa GT, Nathalie S, Livage J (2002) Macroporous crystalline vanadium oxide foam. Nature 416:7777
9. Wang L, Wang W (2012) In situ synthesis of CdS modified $CdWO_4$ nanorods and their application in photocatalytic H2 evolution. CrystEngComm 14:3315. https://doi.org/10.1039/c2ce06656d
10. Yan T, Li L, Tong W et al. (2011) $CdWO_4$ polymorphs: selective preparation, electronic structures, and photocatalytic activities. J Solid State Chem 184:357–364. https://doi.org/10.1016/j.jssc.2010.12.013
11. Xu J, Chen M, Wang Z (2014) Preparation of $CdWO_4$-deposited reduced graphene oxide and its enhanced photocatalytic properties. Dalton Trans 43:3537–3544. https://doi.org/10.1039/c3dt52120f
12. Hou L, Lian L, Zhang L, W T, Y C (2014) Microwave-assisted interfacial hydrothermal fabrication of hydrophobic $CdWO_4$ microspheres as a high-performance photocatalyst. RSC Adv 4:2374–2381. https://doi.org/10.1039/c3ra45784b
13. Lei F, Chen HAOH, Shi Y et al. (2013) Novel preparation method and luminescent properties of Eu^{3+} doped. Adv Mater Res 654:664–668. https://doi.org/10.4028/www.scientific.net/AMR.652-654.664
14. Yue D, Li Q, Lu W et al. (2015) Multi-color luminescence of uniform $CdWO_4$ nanorods through Eu^{3+} ion doping. J Mater Chem C 3:2865–2871. https://doi.org/10.1039/C4TC02409E
15. Wang L, Moon BK, Park SH et al. (2016) Synthesis and photoluminescence of Bi^{3+},Eu^{3+} doped $CdWO_4$ phosphors: application of energy level rules of Bi^{3+} ions. New J Chem 40:3552–3560. https://doi.org/10.1039/C5NJ03058G
16. Rondinone AJ, Pawel M, Travaglini D et al. (2007) Metastable tetragonal phase $CdWO_4$ nanoparticles synthesized with a solvothermal method. J Colloid Interface Sci 306:281–284. https://doi.org/10.1016/j.jcis.2006.10.064
17. Sofronov DS, Sofronova EM, Starikov VV et al. (2012) Microwave synthesis of tetragonal phase $CdWO_4$. Mater Manuf Process 27:490–493. https://doi.org/10.1080/10426914.2011.593229
18. Kingsley JJ, Patil KC (1988) A novel combustion process for the synthesis of fine particle α-alumina and related oxide materials. Mater Lett 6:427–432. https://doi.org/10.1016/0167-577X(88)90045-6
19. Nagabhushana GP, Chandrappa GT (2013) Facile solution combustion synthesis of monoclinic VO_2: a unique and versatile approach. J Mater Chem A 1:11539. https://doi.org/10.1039/c3ta11692a
20. Nagabhushana, Nagaraju, Chandrappa (2013) Synthesis of bismuth vanadate: its application in H_2 evolution and sunlight-driven photodegradation. J Mater Chem A 1:388–394. https://doi.org/10.1039/c2ta00490a
21. You M, Xu J, Zhang Z, Zhou Y (2014) Eu^{3+}-doped $CdWO_4$ phosphor for red-light emission: hydrothermal preparation and blue light excitation. Ceram Int 40:16189–16194. https://doi.org/10.1016/j.ceramint.2014.07.052
22. Yan J, Shen Y, Cao R, Li T (2014) $CdWO_4$ nanorods: ultrafast synthesis via a PEG-1000 polymer-assisted enhanced microwave synthesis route and their photoluminescence property. Ceram Int 40:8081–8085. https://doi.org/10.1016/j.ceramint.2014.01.003
23. Alonso B, Livage J (1999) Synthesis of vanadium oxide gels from peroxovanadic acid solutions: a 51 V NMR study. J Solid State Chem 148:16–19
24. Piquemal J-Y, Briot E, Brégeault J-M (2013) Preparation of materials in the presence of hydrogen peroxide: from discrete or "zero-dimensional" objects to bulk materials. Dalton Trans 42:29–45. https://doi.org/10.1039/c2dt31660a
25. Daturi M, Busca G, Borel MM et al. (1997) Vibrational and XRD study of the system $CdWO_4$-$CdMoO_4$. J Phys Chem B 101:4358–4369. https://doi.org/10.1021/jp963008x
26. Sing KSW, Everett DH, Haul RAW, Moscou L, Pierotti RA, Rouquerol J, Siemieniewska T (1985) International union of pure commission on colloid and surface chemistry including catalysis*Reporting physisorption data for gas/solid systems with special reference to the determination of surface area and porosity. 57:603–619
27. Du Plessis M (2007) Relationship between specific surface area and pore dimension of high porosity nanoporous silicon—model and experiment. Phys Status Solidi Appl 204:2319–2328. https://doi.org/10.1002/pssa.200622237
28. Singh R, Pal B (2013) Study of excited charge carrier's lifetime for the observed photoluminescence and photocatalytic activity of CdS nanostructures of different shapes. J Mol Catal A Chem 371:77–85. https://doi.org/10.1016/j.molcata.2013.01.024
29. Senthil Kumar P, Selvakumar M, Babu SG et al. (2015) Novel CuO/chitosan nanocomposite thin film: facile hand-picking recoverable, efficient and reusable heterogeneous photocatalyst. RSC Adv 5:57493–57501. https://doi.org/10.1039/C5RA08783J